

## PLATINUM-GROUP ELEMENTS IN THE BRAVO INTRUSION, CAPE SMITH FOLD BELT, NORTHERN QUEBEC

SARAH-JANE BARNES AND DANIELLE GIOVENAZZO

*Département des Sciences de la Terre, Université du Québec à Chicoutimi, Chicoutimi, Québec G7H 2B1*

### ABSTRACT

The Bravo intrusion is a komatiitic sill that forms part of a feeder system to the Chukotat komatiitic basalts of the Cape Smith Fold Belt in northern Quebec. The sill is of interest because of the large changes in the distribution of chalcophile and siderophile elements within the intrusion. The differences in their distribution are interpreted to be due to the differences in the history of crystallization, contamination and alteration of each of the zones of the intrusion. The concentrations of the lithophile elements, platinum-group elements (PGE), Ni and Cu in the upper zone of the sill may be modeled as the product of 25% batch partial melting of a fertile mantle, followed by emplacement of this magma into the crust and accumulation of 40 to 60% olivine and 0.5 to 1% sulfide during crystallization. The lithophile elements of the lower-zone rocks may be modeled in a similar manner, but the rocks are much richer in Cu, Ag, Rh, Pt and Pd than most komatiites. This enrichment could have been caused by the contamination of the komatiite magma with a Cu-rich sulfide, which was formed either by partial melting of a pre-existing igneous sulfide or by fractionation of an igneous sulfide liquid. At the base of the intrusion, there is a chlorite-sulfide zone that is depleted in Si, Mg, Ca, Na, K and Cr, and enriched in Ti, Al, REE, Sc, Y and Zr relative to the enclosing komatiite. The Ni, Os, Ir and Ru contents of the sulfide are similar to those found in sulfide associated with komatiites, but the rock is depleted in Pd, Pt and Au, and richer in Cu and Ag than typical komatiite-associated ores. The chlorite-sulfide zone may represent the product of hydrothermal leaching of a komatiite rich in sulfide.

**Keywords:** platinum-group elements, komatiites, Bravo sill, hydrothermal alteration, modeling, Cape Smith Fold Belt, Quebec.

### SOMMAIRE

L'intrusion Bravo est un filon-couche komatiitique faisant partie d'un système nourricier aux basaltes komatiitiques de la ceinture du Cap Smith (Nouveau-Québec). Le filon-couche présente un intérêt particulier puisque la distribution des éléments chalcophiles et sidérophiles varie fortement à l'intérieur de l'intrusion. Ces différences dans leur distribution sont interprétées comme étant le produit de variations dans la cristallisation, la contamination et l'altération de chacune des zones de l'intrusion. La concentration des éléments lithophiles, de ceux du groupe du platine, de Ni et de Cu dans la zone supérieure du filon-couche résulterait de 25% de fusion partielle en masse d'un manteau fertile. Cette fusion fut suivie par l'emplacement de ce magma dans la croûte, ainsi que de l'accumulation de 40 à 60% d'olivine et de 0.5 à 1% de sulfures pendant la

cristallisation. Nous pouvons expliquer les éléments lithophiles des roches de la zone inférieure de la même façon, mais ces roches sont plus riches en Cu, Ag, Rh, Pt et Pd que la plupart des komatiites. Cet enrichissement pourrait avoir été produit par la contamination du magma komatiitique avec des sulfures riches en Cu. Ces derniers auraient été formés soit par une fusion partielle de sulfures ignés pré-existants, soit par le fractionnement d'un liquide igné sulfuré. Une zone à chlorite et sulfures, appauvrie en Si, Mg, Ca, Na, K et Cr, et enrichie en Ti, Al, les terres rares, Sc, Y et Zr par rapport à la komatiite encaissante, se trouve à la base de l'intrusion. Les teneurs en Ni, Os, Ir et Ru des sulfures dans cette zone sont similaires à celles des sulfures associés aux komatiites, mais la roche est appauvrie en Pd, Pt et Au, et enrichie en Cr et Ag, comparée aux minerais typiques associés aux komatiites. La zone à chlorite et sulfures pourrait bien représenter le produit d'un lessivage hydrothermal d'une komatiite riche en sulfures.

**Mots-clés:** éléments du groupe du platine, komatiite, filon-couche de Bravo, lessivage hydrothermal, modèle pétrogénétique, ceinture du Cap Smith, Québec.

### INTRODUCTION

The Cape Smith Fold Belt is an early Proterozoic (1840–2000 Ma, Parrish 1989) fold-and-thrust belt in northern Quebec; it lies between the Archean Superior and Churchill provinces (Fig. 1). The southern half of the belt consists of two stratigraphic groups, the Povungnituk and Chukotat. The Povungnituk Group contains clastic continental-shelf sediments, continental tholeiites and minor alkali basalts, whereas the Chukotat Group consists of basaltic komatiite at the base and mid-ocean-ridge basalt toward the top. These two groups are considered to accompany the opening of a continental rift system (formation of the Povungnituk Group), followed by the development of an ocean (formation of the Chukotat Group: Francis *et al.* 1981, 1983, Hynes & Francis 1982, Picard *et al.* in press).

Ni-Cu sulfides rich in platinum-group elements (PGE) occur in two different stratigraphic settings, known as the Raglan and the Delta horizons (Giovenazzo *et al.* 1989). The Raglan horizon contains the Donaldson, Katiniq and Cross Lake sulfide deposits, which occur at the contact between the Povungnituk Group and the Chukotat Group, within sills or frozen lava lakes of basaltic komatiite composition (Barnes *et al.* 1982, Dillon-Leitch *et al.* 1986,

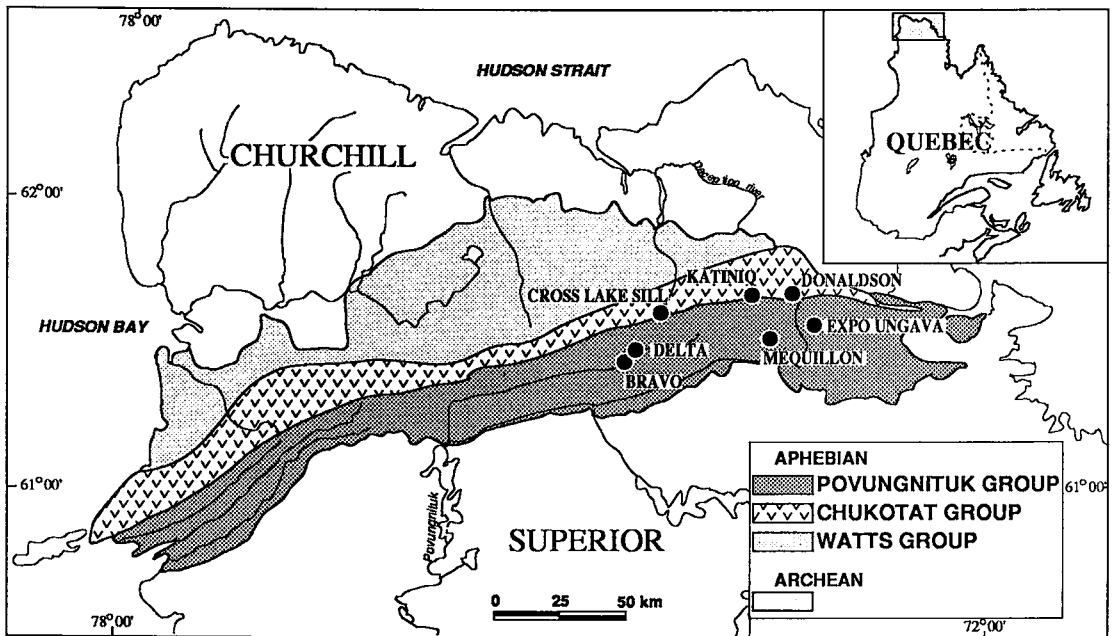


FIG. 1. Location of the sulfide deposits in the Cape Smith Belt. Modified after Giovenazzo *et al.* (1989).

TABLE 1. COMPOSITION OF THE SULFIDE DEPOSITS IN THE CAPE SMITH BELT

Local ity Texture	Ragland Horizon				Delta Horizon						
	Donaldson		Katinic		Cross Lake		Delta Sill		Méquillon		
	Massive	Diss.	Vein	Massive	Diss.	Main	C-1	D-8	D-9	Vein	Diss.
Ref.	1 & 2	1 & 2	1 & 2	3	2	2	2	2	2	2	4
n	5	7	3	4	4	3	2	11	8	1	18
Fe %	49.5	44.1	28.2	49.6	45.7	55.6	55.0	50.9	51.7	36.0	55.7
Ni	9.5	15.2	20.9	10.3	14.2	4.2	5.6	8.6	7.3	15.0	2.8
Cu	0.7	3.1	14.0	1.5	3.7	1.0	1.5	1.2	1.9	10.8	4.5
S	40.2	37.5	36.9	38.5	38.0	39.1	38.0	39.8	39.1	38.5	37.0
Ag ppm	2.2	20	50	-	12.7	-	7.3	-	-	-	-
As	7	47	21	-	<10	2.2	3.5	3.9	2.7	<40	5
Co	1266	2611	1500	-	3045	1467	1467	1971	1548	1531	1382
Cr	<100	<100	274	-	<100	1753	<200	132	333	2871	<100
Sb	2.5	3.8	17.7	-	1.1	1.2	2.2	0.2	1.2	10.6	10.4
Se	80	100	67	-	-	-	-	141	164	-	65
Os ppb	258	432	2	224	477	142	44	73	23	-	43
Ir	200	356	1.7	147	400	169	40	88	23	14.8	75
Ru	1205	1904	25	781	1970	950	213	509	56	85	292
Rh	547	606	12.7	446	273	621	327	535	300	85	963
Pt	2865	5964	752	2561	5489	758	2267	1188	2427	18784	4650
Pd	1572	18229	10096	6191	15620	2847	6553	821	3802	28515	11314
Au	23	115	8436	102	225	65	536	44	34	1988	541

1. Dillon-Leitch *et al.* (1986) 2. Picard & Giovenazzo (in press) and Giovenazzo (in prep)  
3. Barnes *et al.* (1982) 4. Tremblay (1990).

Picard & Giovenazzo, in press). The Delta horizon is made up of the Echo, Bravo, Delta, Méquillon and Expo-Ungava showings (Samis & Andersen 1980,

Daxl 1988, Giovenazzo *et al.* 1989, Tremblay 1990). These sulfide showings occur at the base of ultra-mafic dykes and sills that intrude the upper Povung-

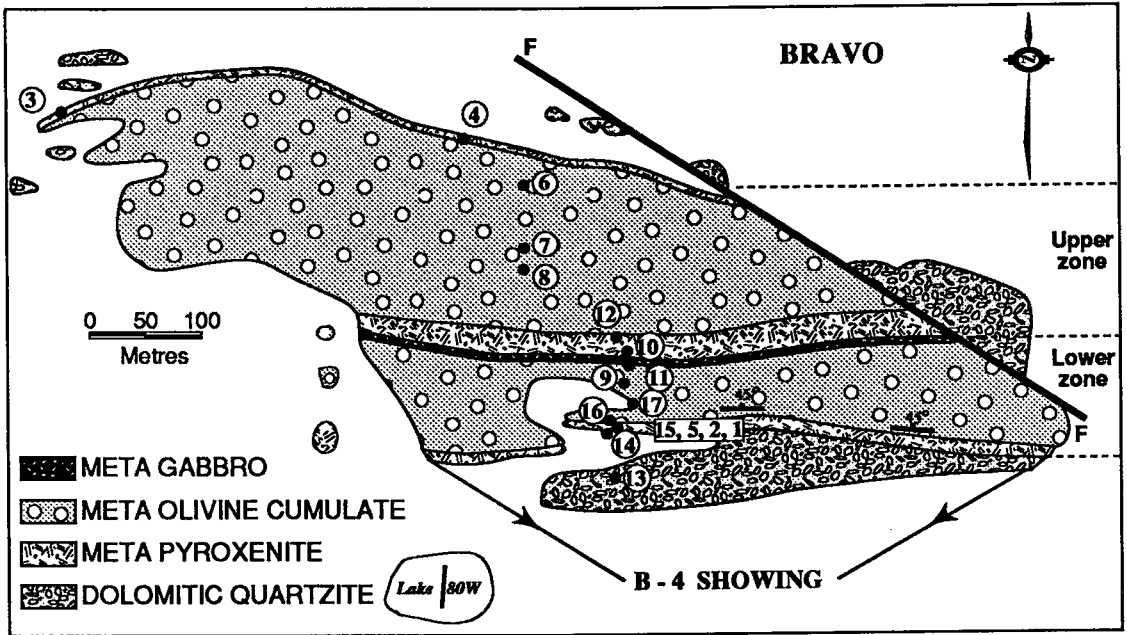


FIG. 2. Sketch map of the Bravo intrusion, showing the location of the samples. Modified after Samis & Andersen (1980).

nituk Group. The distribution of the lithophile elements in the sills suggests that they are comagmatic with the Chukotat Group, *i.e.*, their parent magma was komatiitic basalt (Tremblay & Barnes 1989), but some of the sulfide compositions do not appear to be in equilibrium with a komatiitic basalt (Méquillon and D-9 showings, Table 1). These sulfides tend to have lower Ni/Cu ratios and higher Pd/Ir ratios than those reported for sulfides from the Raglan horizon. The topic of this study is the composition of the sulfides associated with the Bravo intrusion. Our aim is to compare the compositions of the sulfides from the Bravo sill with the sulfides of the Raglan horizon and to explain the distribution and relative abundance of the chalcophile and siderophile elements within the Bravo intrusion.

#### LOCAL GEOLOGY AND PETROLOGY

The Bravo sill is approximately 200 m thick and intrudes dolomitic quartzites of the Upper Povungnituk Group (Fig. 2). Along strike, it is connected to the Echo system of sills to the west and, indirectly, to the Delta sill to the east. The whole system of sills from Echo to Expo-Ungava covers approximately 50 km. The Bravo sill exhibits a zonation typical of the ultramafic sills in the Cape Smith Belt: pyroxenite margins and an olivine mesocumulate core (Bédard *et al.* 1984, Picard 1986). Note that the rocks have experienced greenschist-facies metamorphism, and hence the rock names should be those of meta-

morphic rocks; however, as the igneous textures are well preserved and relict igneous minerals are present, the igneous rock names are used here. Within the intrusion there appear to be two zones (Fig. 2), a lower zone consisting of the basal pyroxenite overlain by the olivine mesocumulate and a thin discontinuous gabbro, and an upper zone consisting of the middle pyroxenite, an olivine mesocumulate, and a capping of the thin border pyroxenite in the north. The sulfide-rich zone, exposed in the B-4 showing,

TABLE 2. ACCURACY AND PRECISION OF THE PGE ANALYSES

	SARM-7	Ax 90	Blank	std. error
	1	2	3	4
	ppb	ppb	ppb	%
Os	55.9	2.3	<0.5	32
Ir	77	2.7	<0.016	8.8
Ru	493	18.6	<3	22
Rh	240	12	<0.1	6.4
Pt	3432	120	<3	26
Pd	1544	338	<2	11
Au	291	5.1	0.15	13.5

1. Results for SARM-7 determined at UQAC
2. The average of 12 runs of the in-house standard AX-90
3. The results using 50 g of quartz instead of sample
4. (one sigma/average) for Ax 90 n=12

TABLE 3. CHEMICAL COMPOSITION OF ROCKS FROM THE BRAVO INTRUSION

Rock	Dv 3	Dv 4	Dv 6	Dv 7	Dv 8	Dv 12	Dv 10	Dv 11	Dv 9	Dv 17	Dv 16	Dv 5	Dv 15	Dv 2	Dv 14	Dv 13	CR 61
SiO <sub>2</sub> %	45.29	45.55	38.25	40.20	38.14	45.47	42.71	50.43	41.40	41.60	40.86	9.56	9.10	18.61	41.78	88.44	56.17
Al <sub>2</sub> O <sub>3</sub>	0.32	0.43	0.10	0.14	0.24	0.30	0.41	0.40	0.28	0.30	0.31	0.46	0.58	0.88	0.38	<0.01	0.44
Fe <sub>2</sub> O <sub>3</sub>	7.17	7.29	2.92	4.20	2.51	8.62	7.93	8.32	4.71	5.58	7.47	6.64	6.41	13.32	7.13	<0.1	11.05
MnO	0.20	0.17	0.16	0.16	0.21	0.17	0.18	0.17	0.19	0.18	0.23	0.20	0.17	0.31	0.21	0.11	0.07
MgO	20.69	21.11	35.03	32.72	32.00	19.72	22.09	14.44	27.30	26.60	19.20	4.80	4.47	10.93	20.69	1.56	4.98
CaO	8.43	8.58	0.55	3.37	2.57	9.13	8.72	15.39	4.46	4.39	7.25	0.40	0.52	0.75	2.65	4.32	2.65
Na <sub>2</sub> O	0.24	0.25	0.02	0.03	0.08	0.37	0.35	0.37	0.18	0.10	0.36	<0.01	<0.01	0.01	0.30	0.03	4.00
K <sub>2</sub> O	0.03	0.02	<0.01	<0.01	<0.01	0.12	0.04	0.12	0.01	0.02	0.04	<0.01	<0.01	<0.01	0.04	0.01	0.62
P <sub>2</sub> O <sub>5</sub>	0.01	0.03	0.01	0.01	0.03	0.01	0.03	0.05	0.02	0.01	0.02	0.02	0.03	0.08	0.03	0.02	4.00
LOI	4.79	4.82	10.71	9.61	9.23	4.38	5.47	1.68	7.70	7.56	3.53	6.00	4.83	4.20	4.66	<0.01	3.16
S	0.02	0.05	0.68	0.01	0.07	0.01	0.05	0.01	0.12	0.24	3.29	24.10	24.50	11.50	2.00	0.09	4.00
Fe(s)	n.d.	n.d.	0.88	n.d.	n.d.	n.d.	n.d.	n.d.	0.17	0.33	3.87	28.35	28.50	12.29	2.23	n.d.	6.88
Ni	0.06	0.09	0.19	0.15	0.13	0.06	0.06	0.04	0.09	0.11	0.26	1.64	1.64	0.64	0.22	<0.01	0.005
Total	99.82	100.01	100.47	100.29	100.26	100.01	100.28	99.51	100.31	99.94	98.55	94.51	93.17	94.73	99.17	99.48	100.895
Ag ppm	<0.5	<0.5	<0.5	<0.5	<0.5	<0.5	<0.5	<0.5	<0.5	<0.5	1.3	8.2	12	9.4	0.8	<0.5	n.d.
As	49.9	35.8	<0.5	<0.5	<0.5	<0.5	<0.5	<0.5	<0.5	1	<0.5	1	2	0.8	<0.5	1.6	n.d.
Co	86.4	77.5	104.3	105.9	132.3	74.8	44.7	44.7	99.7	112	179.7	860	812	325	178.3	2.9	25
Cr	1934	1857	3898	3860	3968	1811	1635	2986	2247	2200	1962	407	435	566	1559	2.9	n.d.
Cu	51	100	264	71	132	22	44	150	252	200	8400	& 5.51	& 5.59	& 4.50	5200	50	300
Fe	<0.2	0.8	<0.2	<0.2	0.6	0.3	0.4	0.28	<0.4	<0.4	0.5	0.6	0.6	1.3	0.54	<0.4	2.8
HP	0.56	0.21	0.59	0.12	0.06	0.14	0.45	0.80	2.2	1.7	1.9	0.50	0.46	0.8	1.5	0.47	0.14
SB	37.3	30.7	15.7	16.8	21.4	32.7	33.4	67.8	26.3	23	26.8	30.5	28.4	38.8	26.8	0.33	10
Sc	<1	<1	<1	<1	<1	<1	<1	2.6	1	<1	10.2	78	76	48	9	<1	3
Se	0.88	0.34	<0.1	<0.1	<0.1	0.1	0.15	<0.1	<0.1	<0.1	1.2	0.82	0.93	<0.1	0.2	11	3
Tb	170	150	140	85	97	142	176	10	118	111	151	180	195	258	146	n.d.	n.d.
V	9	9	<3	<3	<3	9	11	10	7	7	12	n.d.	n.d.	n.d.	10	n.d.	32
Y	83	71	58	67	110	81	64	65	70	64	30	80	79	295	62	27	n.d.
Zn	83	71	58	67	110	81	64	65	70	64	30	80	79	295	62	27	n.d.
Zr	31	33	14	14	17	24	29	35	18	20	26	44	38	60	31	n.d.	133
La ppm	3.02	1.99	0.34	0.63	0.83	1.28	1.33	1.43	1.15	n.d.	1.11	1.35	2.02	3.33	1.28	0.98	50
Ce	4.7	3.5	<2	<2	3.8	3.2	<2	<2	<2	n.d.	3.3	5.44	6.3	8.7	3.0	0.99	103
Sm	1.16	1.28	0.25	0.42	0.58	0.78	1.35	1.27	0.78	n.d.	1.01	1.74	0.90	1.74	0.95	0.20	38
Ru	4.9	5.2	0.32	0.07	0.12	0.28	0.21	0.42	0.28	n.d.	0.26	0.54	0.83	1.34	0.28	0.06	6.8
Rh	1.3	1.9	4.4	1.8	1.7	1.1	1.8	3.8	6.4	6	67.7	648	778	228	42.5	0.1	0.4
Pd	10	9	23	10	11	4.4	8	44	33	62	292	632	910	989	207	1.6	14
Te	9.6	26	52	16	11	4	5	74	129	229	1220	94	114	360	964	<3	17
Au	0.75	0.67	3.13	2.17	2.48	0.68	0.66	0.95	1.20	5	12.34	3.13	2.80	6.59	15.54	0.22	1.4

n.d. = not determined, Fe(s) = Fe present in sulfides.

contains between 5 and 90% sulfide and occurs within the basal pyroxenite. On the surface, it is approximately 3 m wide and 600 m long; diamond drilling indicates that it pinches out at depth (Samis & Andersen 1980).

The pyroxenites consist of subhedral pyroxene grains 2 to 4 mm in size, now replaced by an interlocking mat of actinolite in a matrix of interpenetrating chlorite laths (0.2 mm). In the basal pyroxenite, 5 to 10% disseminated sulfides are interstitial to the pyroxene pseudomorphs in irregular patches that are 2 to 4 mm in diameter and have a narrow (0.1 mm) rim of magnetite. The sulfides consist of anhedral chalcocopyrite and pyrrhotite grains (0.5 mm) with straight boundaries. Exsolution flames of pentlan-

dite occur within the pyrrhotite. Daxl (1988) reported the presence of sperrylite ( $\text{PtAs}_2$ ) and sudburyite ( $\text{PdSb}$ ) as discrete grains in the chlorite.

Within the basal pyroxenite and at the western end of the sill, a 1-m-thick zone rich in chlorite and sulfide is developed. (In the text below, the rocks from this zone are called the chlorite-sulfide rocks). This material has been considered to be of hydrothermal origin (Lamothe *et al.* 1987, Daxl 1988). The sulfides form a matrix containing patches of chlorite 3–5 mm across, which consist of a mat of fine-grained (0.1 mm) interlocking laths. Small (0.025 mm) subidioblastic grains of epidote and titanite are present between the chlorite laths. The sulfides consist of large (1 to 2 cm), irregular patches of either chal-

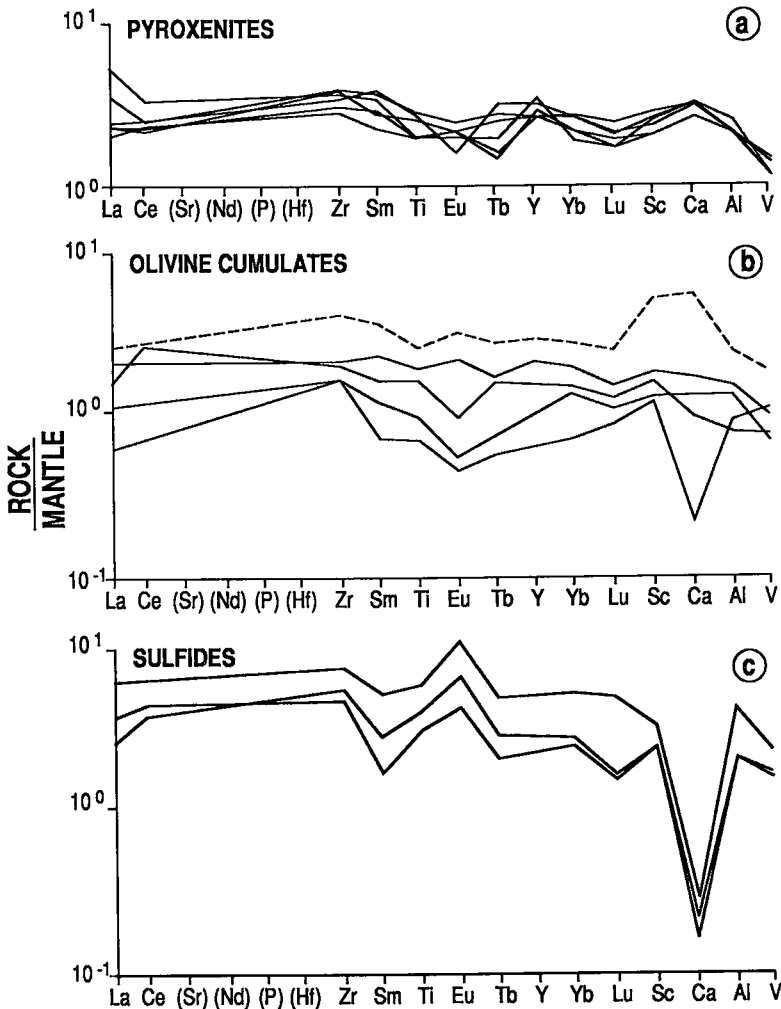


FIG. 3. Mantle-normalized concentrations of incompatible elements in rocks from the Bravo intrusion. Dashed line: gabbro. Normalization values from Taylor & McLennan (1985).

copyrite or pyrrhotite. Exsolution flames of pentlandite occur within the pyrrhotite. The boundary between chalcopyrite and pyrrhotite is lobate, and small inclusions of chalcopyrite occur within the pyrrhotite and *vice versa*. None of the minerals in this zone appears to have a preferred orientation.

The olivine mesocumulate contains anhedral oikocrysts of augite 0.5 to 1 cm across, now partly replaced by laths of actinolite and hornblende. The medium-grained (1 to 2 mm) tabular to polyhedral

olivine chadacrysts within the augite have been replaced by a combination of serpentine, chlorite and magnetite. Interstitial to the oikocrysts are 1-mm patches of sulfides and a chlorite mat. The sulfides consist of pyrrhotite with inclusions of chalcopyrite and exsolved pentlandite. In some samples, the sulfides are partly replaced by magnetite. Small (0.2 mm) euhedral grains of chromite occur within the pyroxene, the sulfides and the chlorite matrix.

The gabbro has a coarse-grained (5 mm) ophitic texture. The pyroxene laths have been replaced by actinolite, and the plagioclase, by a mixture of chlorite and epidote.

#### GEOCHEMISTRY

##### Analytical methods

The major elements, except for Na, and the trace elements Ag, Cu, Ni, S, V, Y and Zr, were determined by X-ray-fluorescence analysis (XRF) at Midland Earth Science Laboratories, Merseyside, U.K. All other analyses were carried out at the Université du Québec, Chicoutimi (UQAC). The platinum-group elements and Au were preconcentrated in a Ni-sulfide bead using the method of Robert *et al.* (1971). The bead was then dissolved, and the noble metals were collected on filter paper, which was then irradiated. The concentrations of the noble metals were determined by instrumental neutron-activation analysis (INAA). The remaining trace elements and Na were determined by INAA on 2 g of rock powder. As a cross-check on the accuracy of the XRF analyses and the recovery of the Ni-sulfide bead technique, Fe, Ir and Au were also determined on the 2 g of rock powder. The difference between Fe determined by XRF and by INAA was less than 5%, and the difference between Ir and Au determined from the filter paper and Ir and Au determined on the rock powder by INAA was less than 15%. An estimate of the accuracy and precision of PGE results is listed in Table 2.

##### Distribution of the lithophile elements

The pyroxenite samples (BV3, 4 and 10) show no cumulate textures and are assumed to approximate the composition of the liquid. The Mg concentrations cover the range 20 to 22% MgO (Table 3), which is a little higher than the highest concentrations (19%) recorded for the overlying komatiitic basalts, which the Delta horizon intrusions are believed to feed (Francis *et al.* 1981, 1983, Giovenazzo *et al.* 1989, Picard *et al.* in press). It is possible to explain the lower Mg contents of the lavas relative to that of the sills by fractionation of 5 to 10% olivine in the conduits, which lowered the Mg content of lavas prior to eruption.

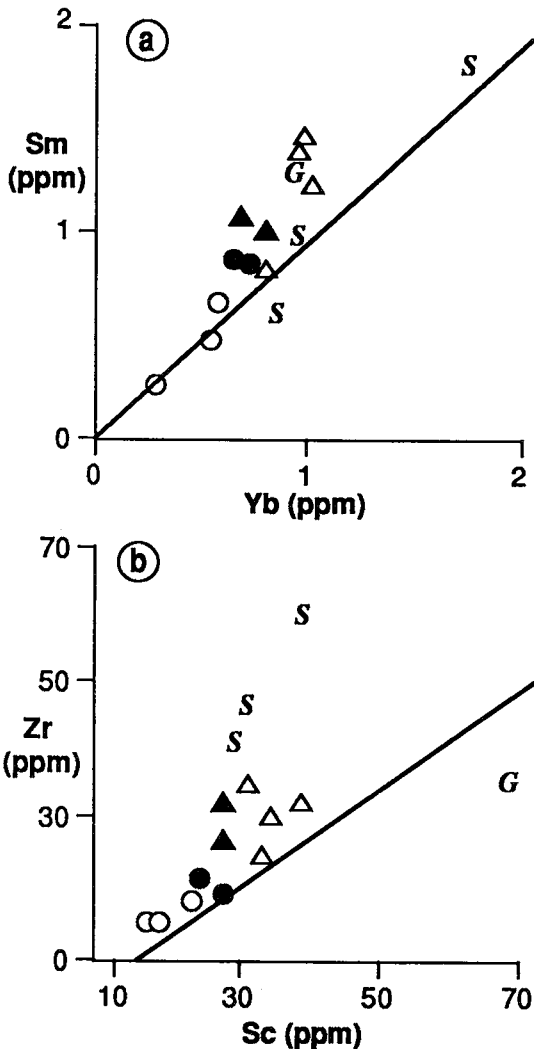


FIG. 4. Sm versus Yb (a) and Zr versus Sc (b). Triangles: pyroxenite, circles: olivine cumulate, G: gabbro, S: sulfide-chlorite rock, open symbols: upper zone, solid symbols: lower zone. Note that the samples plot above the chondrite line (solid line), which indicates that they are enriched in Sm and Zr relative to Yb and Sc, possibly owing to garnet retention at the source.

The ratios between elements from the group La, Sm, Ti and Zr and elements from the group *HREE*, Y, Sc, V, Al are greater than chondritic; for example,  $La/Lu_n = 1.6$ ,  $Zr/Y_n = 1.3$ ,  $Ti/Al_n = 1.2$ ,  $Sm/Sc_n = 1.3$ , as illustrated on mantle-normalized plots of incompatible elements (Fig. 3a). The same point is illustrated on the plots of Sm versus Yb and Zr versus Sc (Figs. 4a, b), where the samples plot on the Sm- and Zr-enriched side of the chondrite line. The level and shape of the patterns are similar to those for the overlying komatiitic basalts (Francis *et al.* 1983, Picard *et al.* in press), which indicates that the Bravo intrusion and the komatiitic basalts could be comagmatic.

Pyroxenites of the lower zone (BV14 and 16) contain cumulate sulfide and olivine. The presence of these cumulate phases does not change the incompatible element ratios; thus the mantle-normalized patterns of the lower pyroxenites are indistinguishable from those of the upper-zone pyroxenites (Fig. 3a), which suggests that these pyroxenites also formed from a komatiitic magma.

Owing to the presence of cumulate olivine, the cumulates contain higher concentrations of Fe, Mg, Ni and Co than the pyroxenite margins (Table 3). They also contain higher concentrations of Cr, which indicates that either some chromite or pyroxene accumulated in the olivine cumulate. As mentioned in the section on petrography, euhedral chromite and augite oikocrysts are present the olivine cumulate, but it is not possible on textural grounds to distinguish between chromite and augite crystallized from trapped liquid and cumulate chromite and pyroxene. However, the plots of  $SiO_2$  and CaO versus MgO (Figs. 5a, b) show that the olivine cumulates and pyroxenites lie on olivine control lines rather than olivine + pyroxene control lines, and there is no evidence for pyroxene as a cumulate phase. Therefore, the higher Cr content in the olivine cumulates is attributed to the presence of cumulus chromite. The concentrations of incompatible elements are diluted by the cumulate phases, but the interelement ratios are similar to those of the pyroxenite, and the mantle-normalized patterns are parallel to those of the pyroxenite, except for some negative Eu and Ca anomalies (Fig. 3b). The similarity of the mantle-normalized patterns of the olivine cumulate and pyroxenite indicates that the trapped liquid component in the cumulates is similar in composition to that of the pyroxenite.

The gabbro sample has mantle-normalized patterns that are parallel to the pyroxenite and the olivine cumulate, except that it shows enrichments in Sc and Ca (Fig. 3b). The similarity of the trace element patterns is consistent with the derivation of the gabbro from the magma that formed the pyroxenites and olivine cumulates. The gabbro has a lower Mg content and higher Si content than the presumed ini-

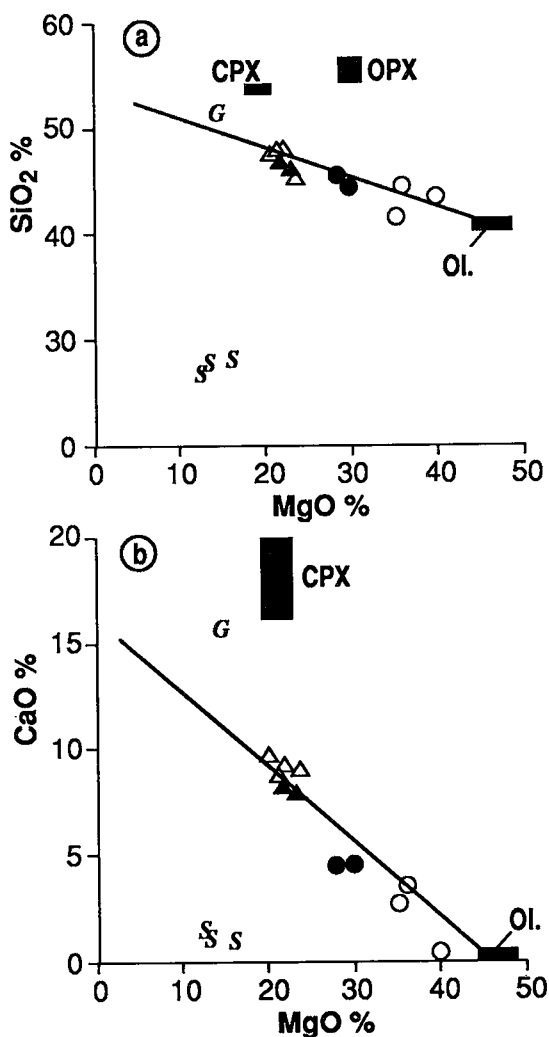


FIG. 5.  $SiO_2$  (a) and CaO (b) versus MgO; legend as in Fig. 4. The ranges in compositions shown for the olivine, clinopyroxene and orthopyroxene shown are those calculated to be in equilibrium with the initial liquid and the liquid after fractionation of 30% olivine, using the equations of Nielsen (1985) and Jones (1984). Note that apart from the gabbro and chlorite-sulfide rocks, the samples plot along olivine control lines and do not show the influence of pyroxene fractionation.

tial magma, which indicates that some olivine fractionation occurred before this rock formed (Fig. 5a). However, the gabbro does not simply represent a fractionated liquid, because on the CaO versus MgO plot the gabbro does not lie on the olivine control line but rather on the clinopyroxene control line. Thus the gabbro may represent a clinopyroxene cumulate with fractionated trapped liquid. The

presence of cumulate clinopyroxene also would explain the Sc enrichment in this sample.

As the chlorite-sulfide rocks occur within the basal pyroxenite, it is possible that the original rock was a sulfide-rich pyroxenite. The mantle-normalized patterns of the chlorite-sulfide rocks (Fig. 3c) are similar to those of the pyroxenites, except for the presence of large negative Ca anomalies and large positive Eu anomalies. Thus the incompatible elements support the idea that the protolith of the chlorite-sulfide rocks was the pyroxenite.

#### Numerical modeling of the lithophile elements

It is possible to model both the major and trace elements of the pyroxenite by 25% batch partial melting of a fertile mantle (Table 4). The degree of partial melting was estimated by considering the high-field-strength elements and assuming that the partition coefficient for these elements into the resid-

uum was zero; thus the batch partial melting equation reduces to:

$$C_s/C_l = 1/F \quad (1)$$

where  $C_s$  and  $C_l$  are the concentration of the element in the mantle and the magma, respectively, and  $F$  is the degree of partial melting.

The enrichment of Zr, Sm and Ti over HREE, Y, Sc indicates that garnet may have been a residual phase during partial melting. If so, then the melting event should have taken place at pressures of greater than 30 kbar, and the other residual phases would have been olivine and low-Ca pyroxene (Takahashi 1986). The weight fraction of each of these phases present in the residuum can be calculated by using the composition of the minerals listed by Takahashi (1986) and by simultaneously solving equation 2, which is a simple mass-balance equation, for  $\text{SiO}_2$ ,  $\text{Al}_2\text{O}_3$ , FeO and MgO:

$$W_o C_o + W_p C_p + W_g C_g = (C_s - C_l F)/(1-F) \quad (2)$$

where  $W_o$ ,  $W_p$  and  $W_g$  are the weight fraction of olivine, pyroxene and garnet, respectively, and  $C_o$ ,  $C_p$  and  $C_g$  are the concentrations of oxides in olivine, clinopyroxene and garnet, respectively.

The "observed initial liquid", based on the average of the pyroxenites, and the modeled melt show reasonable agreement (Table 4), except for Ca, Na, K and Eu concentrations. Calcium, Na, K and Eu have all been shown to be mobile in metamorphosed komatiite (Sun & Nesbitt 1978, Beswick 1982, Ludden *et al.* 1983), and therefore the lack of agreement for these elements is not considered surprising.

In order to model the composition of the cumulate rocks, it is necessary to estimate how much trapped liquid component is present and to evaluate its degree of fractionation. The amount of trapped liquid present may be estimated by considering an incompatible element and using the equation:

$$T = C_c/C_l \quad (3)$$

where  $T$  is the weight fraction of the trapped liquid, and  $C_c$  and  $C_l$  are the concentrations of the element in the cumulate and liquid, respectively. If the trapped liquid component has the same composition as the initial magma, then  $C_l$  will be lower, and hence the  $T$  higher, than if the trapped liquid component is fractionated. Therefore, to estimate how much trapped liquid component is present, it is necessary to estimate the degree of fractionation of the liquid. Where olivine is the cumulate phase, use of a plot of  $\text{MgO}/(\text{MgO} + \text{FeO})$ , all in wt.%, versus an incompatible element leads to an estimation of the degree of fractionation of the trapped liquid component. On such a plot, tie lines between the ini-

TABLE 4. MODEL MELT COMPARED WITH ESTIMATED LIQUID

	Initial Liquid	Model Melt	Fertile Mantle	Restite Olivine	Minerals Pyx.	Garnet
	1.	2.	3.	4.	4.	4.
$\text{SiO}_2$ %	47.64	47.99	44.48	40.28	52.83	42.03
$\text{TiO}_2$	0.41	0.51	0.16	0	0.14	0.18
$\text{Al}_2\text{O}_3$	7.98	7.92	3.59	0.19	6.15	22.21
FeO	11.67	12.69	8.10	7.22	4.40	4.83
MnO	0.19	0.17	0.12	0.10	0.12	0.17
MgO	22.50	23.62	39.22	50.94	24.80	22.65
CaO	9.17	6.51	3.44	0.29	9.05	5.10
$\text{Na}_2\text{O}$	0.29	0.61	0.30	0	0.74	0.04
$\text{K}_2\text{O}$	0.03	0.08	0.02	0	0	0
				Partition Coefficients <sup>5</sup>		
Ag ppm	<0.5	0.15	0.019	0	0	0
As	29	0.4	0.10	0	0	0
Co	84	100	100	1	1	0
Cr	1900	1400	3000	0.5	8	15
Cu	69	112	28	0	0	0
Hf	1.1	1.1	0.27	0	0	0
La	2.2	2.2	0.55	0	0	0
Ni	650	616	2000	4	1	0.8
Lu	0.13	0.14	0.057	0	0.2	7
S	400	800	200	0	0	0
Sb	0.42	0.1	0.025	0	0	0
Sc	35	23	13	0	0.5	6.5
Se	<1	0.16	0.041	0	0	0
Sm	1.33	1.2	0.347	0	0.25	0.08
V	173	156	128	0	2	8
Y	10	11	3.4	0	0.2	1.4
Zn	76	61	50	1	0.3	0.3
Zr	32	33	8.3	0	0	0
Os ppb	0.9	0.9	5	D bulk = 7.5		
Ir	0.8	0.8	4.4	D bulk = 7.5		
Rh	1.7	1.6	1.6	D bulk = 1		
Pt	9.5	8.3	8.3	D bulk = 1		
Pd	14	17	4.4	0	0	0
Au	0.7	4.8	1.2	0	0	0

1. Average of upper-zone pyroxenites by 3, 4 and 11
2. Model melt assuming 25% batch partial melting of a fertile mantle, leaving a restite of 75% olivine 22.5% low-Ca pyroxene, and 2.5% garnet.
3. Fertile mantle composition, major elements based on KLB-1 (Takahashi 1986), trace elements from Taylor & McLennan (1985) PGE from Barnes *et al.* (1988).
4. Olivine, low-Ca pyroxene and garnet compositions in equilibrium with melt at 1550 C and 30 Kbar.
5. Partition coefficients used from Irving (1978), for silicates and Naldrett & Barnes (1986) for sulfide.

tial liquid and the olivine in equilibrium with it can be drawn using the relationship  $(\text{FeO}/\text{MgO})_{\text{ol}}/(\text{FeO}/\text{MgO})_{\text{liq}} = 0.3$  (Roeder & Emslie 1970). Any rock that consists of initial liquid plus olivine should lie on a tie-line between the two. As olivine is removed from the liquid, the liquid and the olivine in equilibrium with it become more Fe-rich, and the tie-line moves. Tie-lines for 10, 20 and 30% olivine fractionation are shown on Figure 6. The presence of sulfide will not disturb the coordinates of a rock provided that the Fe in the sulfide is not included in the "FeO". Using this method, it is possible to estimate that the cumulate rocks at Bravo have experienced fractionation of between 10 and 30% olivine prior to their formation. It is possible to model the distribution of lithophile elements in the olivine cumulates as liquid plus 40 to 60% olivine and 1% chromite (Table 5). The basal pyroxenites appear to be unfractionated (Fig. 6) and can be modeled as consisting of 90% initial liquid plus 5% olivine and 5% sulfide (Table 5). The gabbro sample may be modeled as the fractionated liquid plus 20% cumulate clinopyroxene, but the match between the model and observed compositions is poor for CaO and FeO, either because the equations used to estimate the composition of the clinopyroxene are not correct or because the gabbro is not directly derived from the initial magma. As this intrusion is part of an open system, the gabbro may have crystallized from another batch of magma.

In the case of the chlorite-sulfide rock, the similarity in the shape of the incompatible element patterns (Fig. 3) indicates that the protolith could have been the pyroxenite. In terms of the major oxides, the composition of the silicate portion of the chlorite-sulfide rock is close to that of a chlorite (Table 6), which is consistent with the petrographic observations. If this rock has been derived from the pyroxenite, then large amounts of Si, Mg, Ca and Na must have been removed from it. The net loss or gain of an element may be calculated by

$$D = (C_s 0.39 - C_p) / C_p 100 \quad (4)$$

where D is the percentage loss or gain of the element,  $C_p$  and  $C_s$  are the concentrations of the element in the pyroxenite and chlorite-sulfide rock, respectively, the constant 0.39 allows for the volume change in the rock, estimated by assuming that Ti and Al were immobile and taking the average of  $\text{Ti}_p/\text{Ti}_s$  and  $\text{Al}_p/\text{Al}_s$ . The results of this calculation indicate that if the chlorite-sulfide rock formed from the pyroxenite, then the silicate portion of the rocks has lost 61% of its original weight, mainly by loss of Si, Mg, Ca, Na, K and Cr (Table 6). This is considered reasonable, since all of these elements except Cr are fairly mobile; the immobile elements show much smaller changes.

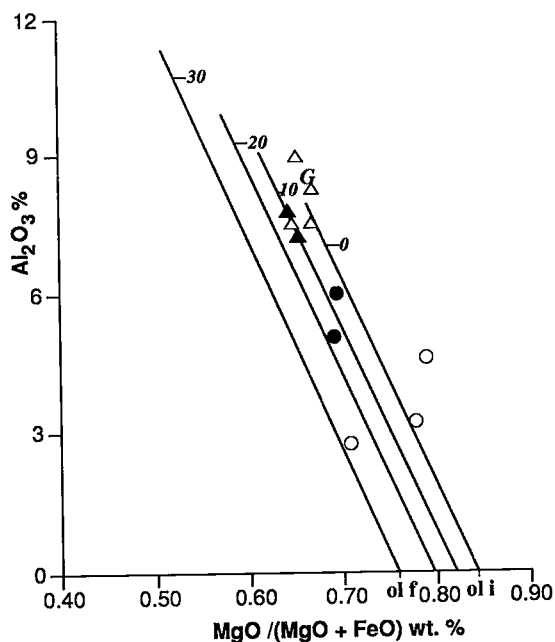


FIG. 6.  $\text{Al}_2\text{O}_3$  versus  $\text{MgO}/(\text{MgO} + \text{FeO})$ , all in wt.%; legend as in Fig. 4. Solid lines represent tie-lines between the liquid and the olivine calculated to be in equilibrium with the liquid, calculated using the Roeder & Emslie (1970) equation for fractionation of 0, 10, 20 and 30 wt. % olivine. The initial liquid composition is listed in Table 4.

#### *Distribution of the chalcophile and siderophile elements*

The PGE, Au, Ni and Cu contents of the upper-zone pyroxenite are intermediate between those previously reported for komatiites and komatiitic basalts (Munro Township in Ontario, the Yilgarn Block of Western Australia and the Karasjok Greenstone Belt of northern Norway: Crocket & MacRae 1986, Brüggmann *et al.* 1987, Keays 1982, Barnes & Often 1990). On metal ratio plots of Ni/Cu versus Pd/Ir (Fig. 7), they straddle the boundary between the fields komatiites and high-Mg basalts (which includes komatiitic basalts). The Munro, Yilgarn and Karasjok komatiites contain from 25 to 30% MgO, and the komatiitic basalts contain from 12 to 16% MgO. The Mg content of the Bravo pyroxenites is in the range 20 to 22% MgO; thus the intermediate PGE, Au, Ni and Cu contents of these pyroxenites are consistent with their Mg content.

The mantle-normalized metal patterns of the upper-zone olivine cumulates are slightly higher than those of the pyroxenite (Fig. 8a) but parallel to them, which may be attributed to the presence of a small

TABLE 5. MODELS OF THE CUMULATE ROCKS OBTAINED BY RAYLEIGH FRACTIONATION

	Upper Zone		Lower Zone			Mineral Compositions					
	oC	oC	oC	Pyx	Gabbro	Olivine	Chromite	Clinopyroxene	Sul		
	1	2	3	4	5	6	7	8	9	10	11
SiO <sub>2</sub> %	44.26	42.70	45.07	42.97	50.37	41.01	40.05	0	55.37	54.15	0
TiO <sub>2</sub>	0.19	0.15	0.27	0.37	0.59	0	0	0	1.03	1.13	0
Al <sub>2</sub> O <sub>3</sub>	3.90	3.03	5.61	7.18	8.85	0	0	15.09	0.69	1.29	0
FeO	10.12	9.65	12.10	10.93	11.32	8.7	13.74	23.92	5.25	5.94	0
MnO	0.17	0.18	0.16	0.17	0.15	0.17	0.17	0	0.17	0.17	0
MgO	36.28	38.20	28.96	22.72	14.39	49.43	45.22	11.12	22.73	18.65	0
CaO	4.47	3.48	6.91	8.25	13.69	0	0	0	16.00	19.94	0
Na <sub>2</sub> O	0.14	0.11	0.19	0.26	0.30	0	0	0	0.06	0.06	0
K <sub>2</sub> O	0.03	0.01	0.00	0.00	0.01	0	0	0	0.00	0.00	0
Fe(s)				2.35							
						Partition	Coefficients				
Ag ppm	0.18	0.38	0.29	0.75	0.7	0	0	0			2000
As	0.48	0.9	0.72	2.4	1.8	0	0	0	0	0	2000
Co	92	109	94	85	92	1	4	1			20
Cr	4465	4000	1683	1710	3658	0.5	49.8	8			0
Cu	64	157	107	354	191	0	0	0			1300
Hf	0.52	0.42	0.43	0.99	1.1	0	0	0			0
La	1.03	0.83	0.87	1.94	2.2	0	0	0			0
Ni	1469	2000	1066	3250	466	4	50	1			890
Lu	0.06	0.05	0.09	0.12	0.14	0	0	0.2			0
S	1850	6000	2400	20000	3900	0	0	0			-
Sb	0.48	0.9	0.16	0.5	0.45	0	0	0			2000
Sc	21	14	31	32	67	0.25	0	3			0
Se	0.19	0.34	0.29	0.8	0.7	0	0	0			2000
Sm	0.62	0.50	0.9	1.2	1.3	0	0	0			0
V	80	65	112	153	261	0	0	2			0
Y	4	4	6.7	9	10	0	0	0.2			0
Zn	76	76	76	76	76	1	2	0.3			0
Zr	15	12	21	29	32	0	0	0			0
Ir ppb	1.8	3.0	1.6	4.8	0.9	2	0	0			20000
Rh	2.0	4.4	3.3	10	7.7	0	0	0			20000
Pt	10.4	22	16.7	50	43	0	0	0			20000
Pd	18	40	28	85	66	0	0	0			20000
Au	0.85	2.3	3.3	4.1	3.1	0	0	0			20000

1. Model of bv 7, consisting of 47% initial liquid (Table 4, column 1), 52% olivine, 1% chromite and 0.5% sulfides.
2. Model of bv 6; 60% olivine, 1% chromite, 1.9% sulfides and 38% initial liquid.
3. Model of bv 9 or 17, consisting of 46.4% olivine, 0.6% sulfide 53% fractionated liquid (19.6% olivine and 0.4% chromite removed).
4. Model of bv 14, consisting of 5% olivine and 5% sulfide and 90% initial liquid.
5. Model of bv 11, consisting of 20% clinopyroxene, 1% sulfides and 79% fractionated liquid (29.4 % olivine and 0.6% chromite removed).
6. Olivine composition in equilibrium with the initial liquid (Roeder & Emslie 1970).
7. Olivine composition in equilibrium with the magma after 30% olivine fractionation
8. Chromite composition based on probed compositions.
9. Clinopyroxene in equilibrium with the liquid after 30% fractionation (Nielsen 1985).
10. Clinopyroxene in equilibrium with the liquid after 40% fractionation (Nielsen 1985).
11. Sulfide partition coefficients from Peach et al. (1989)

amount of cumulate sulfide. The composition of the sulfide component was calculated from sample BV6, which contains the most sulfide (Table 7). The upper-zone sulfide at Bravo is similar to that observed for the massive ore in the nearby Delta D-8 zone, but contains less Cu, Pt, Pd and Au than the sulfide from the Méquillon showing (Table 1). Compared with sulfides from the Raglan horizon, the upper-zone sul-

fide is poorer in Ni, Cu, and PGE than the Donaldson and Katiniq deposits, and similar to the Cross Lake showing (Table 1).

The upper-zone rocks plot close to the tie-line between initial liquid and sulfide of similar composition to the BV6 sulfide on the plot of Ir versus Rh (Fig. 9). Two of the olivine cumulate samples plot on the Ir-enriched side of the tie-line, which indicates

that some Ir is present in the cumulate phases.

In contrast to the lithophile elements, concentrations of the PGE, Au, Ni and Cu in the lower-zone pyroxenite, olivine cumulate and gabbro are very different from those of the upper-zone rocks. The concentrations of these elements are 5 to 100 times higher in the lower-zone rocks. The higher concentrations can be attributed in part to the presence of the sulfide. However, not only are the concentrations higher, but also the interelement ratios are markedly different. The mantle-normalized metal plots for the lower-zone rocks are much steeper than those of the upper zone (*cf.* Figs. 8a, b). The Pd/Ir ratio is an order of magnitude higher in the lower-zone rocks than in the upper-zone rocks, whereas the Ni/Cu ratio is an order of magnitude lower. Thus on the metal ratio plot (Fig. 7), the lower-zone samples tend toward the flood basalt field. These high Pd/Ir (190) and low Ni/Cu (0.3) ratios are unusual for sulfides related to komatiites or basaltic komatiites, which generally have Pd/Ir and Ni/Cu ratios of 5 to 20 (Naldrett 1981). In particular, the sulfide at Katinig, Donaldson, Cross Lake and the Delta D-8 zone all have Pd/Ir ratios in the range 5 to 50, and Ni/Cu ratios of 4 to 10 (Table 1). High Pd/Ir ratios are found in the Cross Lake C-1 showing, the Delta D-9 zone and the Méquillon Sill (Table 1). However, none of the rocks have Ni/Cu ratios as low as the lower-zone sulfides at Bravo. The reason for the high Pd/Ir and low Ni/Cu ratios in the lower rocks at Bravo is the unusually high Cu and Pd concentrations (Table 7). In addition to the high Cu and Pd concentrations, the sulfide is rich in Pt, Rh, Ag, Sb and Se. As can be seen on Figure 9, the lower-zone rocks are distinctly Rh-enriched relative to the upper-zone rocks.

The composition of the sulfide in the chlorite-sulfide rocks is similar to that of the lower zone, except that the chlorite-sulfide rocks have much lower concentrations of Pt, Pd, Au and Sb (Table 7). The mantle-normalized metal patterns for the chlorite-sulfide rocks are similar to those of the other lower-zone rocks, except that they have large negative Pt, Pd and Au anomalies (Fig. 8c). On the plot of Ni/Cu versus Pd/Ir, the chlorite-sulfide rocks fall outside the range of igneous rocks (Fig. 7). Igneous rocks with such low Ni/Cu ratios normally have high Pd/Ir ratios. The fact that considerable amounts of the mobile lithophile elements have been lost from these chlorite-sulfide rocks suggests the possibility that Pt, Pd, Au and Sb, which are all considered to be relatively mobile (Westland 1981, Wood *et al.* 1990), also have been removed. The fluid that removed these elements did not remove Ag and Cu, however. A fluid containing "hard" ligands, such as chlorine, which bond strongly to Ag and Cu, would therefore not be suitable to cause the alteration, but a solution containing "soft" ligands, such as thiosul-

TABLE 6. COMPARISON OF THE SILICATE PORTION OF THE SULFIDE-CHLORITE ROCK WITH THE PYROXENITE

	Chlorite	Pyroxenite	wt % dif
	1.	2.	3.
SiO <sub>2</sub> %	24.27	47.64	- 80.1
TiO <sub>2</sub>	1.28	0.41	+ 21.7
Al <sub>2</sub> O <sub>3</sub>	17.11	7.98	- 16.3
Fe <sub>2</sub> O <sub>3</sub>	30.56	12.98	- 8.1
MnO	0.48	0.19	- 1.4
MgO	12.83	22.50	- 77
CaO	1.11	9.17	- 95
Na <sub>2</sub> O	<0.01	0.29	-100
K <sub>2</sub> O	<0.01	0.03	-100
P <sub>2</sub> O <sub>5</sub>	0.08	0.03	+ 4
H <sub>2</sub> O	10.99	-	
La ppm	4.3	2.2	- 23.7
Ce	13.8	4.2	+ 28
Sm	2.3	1.3	- 31
Eu	1.7	0.29	+128
Tb	0.5	0.25	- 22
Yb	2.2	0.98	- 12
Lu	0.26	0.13	- 22
Cr	970	1900	- 80
Hf	2.9	1.1	+ 2.8
Sc	67	35	- 25
Th	2	0.47	+ 65
V	435	173	- 1.9
Zn	274	76	+ 40
Zr	96	32	+ 17

1. Average of the silicate portion of bv 2, 5 and 15. 2. Average of the pyroxenites bv 3, 4 and 10. 3. The difference between the silicate portion of the chlorite-sulfide rock and the pyroxenite expressed as a wt % loss or gain

fate or bisulfide, would (Seward 1973, Phillips & Groves 1983, Wood *et al.* 1990).

The loss of Pd, Pt, Au and Sb from the chlorite-sulfide rocks offers a solution to the problem of the high concentration of these elements in the other lower-zone rocks, namely that they have been introduced hydrothermally from the chlorite-sulfide rocks. The high Pd/Ir ratio and Cu-rich nature of the disseminated sulfide in the lower-zone pyroxenite support the idea of hydrothermal redistribution of Cu and Pd, since hydrothermal sulfides have high Pd/Ir ratios and high Cu contents (Rowell & Edgar 1986, Leshner & Keays 1984). However, compared with hydrothermal veins of the Donaldson and Delta deposits, the lower-zone sulfide at Bravo is rich in

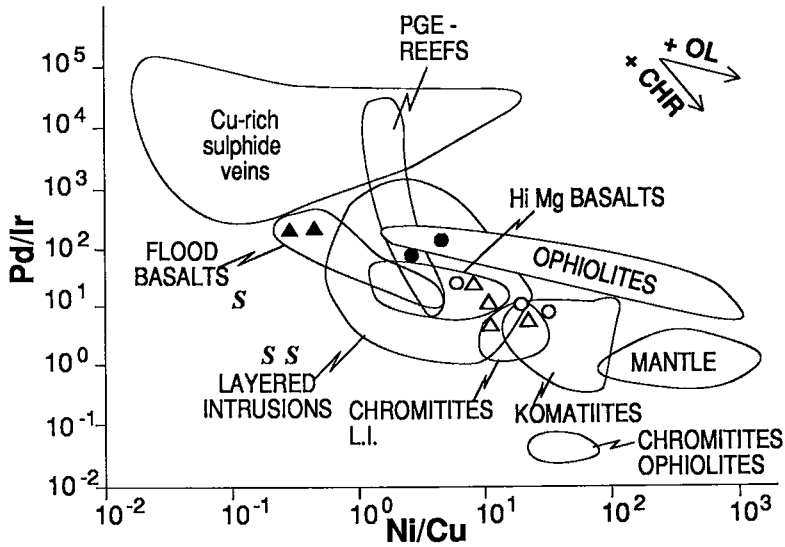


FIG. 7. Pd/Ir versus Ni/Cu, legend as in Fig. 4. L.I.: layered intrusion, fields from Barnes *et al.* (1988). Note that the lower-zone samples fall in the komatiite or high-Mg basalt field; the upper-zone samples are more fractionated, but still fall in the field of igneous rocks, whereas the sulfides fall outside all known fields.

the immobile *PGE* Os, Ir, Ru and Rh (Table 7) and poor in the mobile elements Ag, As and Au. Furthermore, the sulfide is present not in veins but rather disseminated among the pyroxene grains, which suggests an igneous rather than hydrothermal texture. Whereas redistribution of Pt, Pd and Au from the chlorite-sulfide rocks to lower-zone rocks could account for the Pt- and Pd-rich nature of these rocks, it will not solve the problem of the high concentrations of Rh, Ag and Cu in both the chlorite-sulfide rocks and the other lower-zone rocks. As can be seen on Figure 9, all of the lower-zone rocks are enriched in Rh relative to the upper zone. If the hydrothermal redistribution of Pd, Pt, As and Sb from the chlorite-sulfide rocks to the other lower-zone rocks accounts for the high concentration of these elements in the lower-zone rocks, it is still necessary to postulate the introduction of Rh, Cu and Ag from some outside source. This hypothesis is not attractive because it requires the mobility of Rh, which is generally considered to be immobile (Plimer & Williams 1988). Therefore, whereas the chlorite-sulfide rocks may have formed by hydrothermal alteration of a sulfide-rich pyroxenite, with the loss of Pd, Pt, Au, Si, Mg, Ca and the alkalis, hydrothermal alteration will not account for the Rh-, Pt- and Pd-rich nature of all of the lower-zone sulfides.

#### *Numerical modeling of the chalcophile and lithophile elements*

The concentrations of the chalcophile and sidero-

phile elements in the upper-zone pyroxenites may be modeled, like the lithophile elements, as the result of batch partial melting of a fertile mantle. The most important phase in controlling *PGE* is sulfide, but at 25% partial melting, no sulfide would be present in the residuum (Morgan 1986, Barnes 1987); therefore, Pd may be treated as an incompatible element during batch partial melting. The modeled and observed Pd contents are in reasonable agreement (Table 4, columns 1 and 2). Os and Ir behave in a compatible fashion during partial melting (Crocket 1981, Naldrett & Barnes 1986), but the partition coefficients into the various phases are unknown. However, by the use of a bulk-partition coefficient of 7.5, the Os and Ir contents of the upper-zone pyroxenite can be modeled. If Ru, Rh and Pt are treated as incompatible elements, then the model values would be approximately twice the observed values; a bulk partition-coefficient of 1 into the source is required for the modeled and observed values to agree. Naldrett & Barnes (1986) found that the compatibility of Rh is intermediate between Ir and Pd for a range of magmas. The Bravo data suggest that Ru and Pt also show an intermediate degree of compatibility. The observed Au and S concentrations are much lower than those estimated by the model, whereas the observed As and Sb concentrations are much higher than those of the model. The poor agreement between the model and observed concentrations for these elements could reflect poor estimates of the concentration of the elements in the mantle, but given the fact that the rocks have been

metamorphosed to middle-greenschist facies, it more likely reflects mobility of these elements.

The presence of a small amount of cumulate sulfide in the olivine cumulates of the upper zone is indicated by the slightly higher concentrations of PGE in these rocks than in the pyroxenites that are assumed to represent the initial liquid. The composition of the sulfide that forms from a magma is strongly influenced by the amount of sulfide that segregates (the  $R$  factor of Campbell & Naldrett 1979). By rearranging the standard equations for crystal fractionation, the relation between the composition of the sulfide and the amount of sulfide that has segregated may be described by:

$$C_c/C_l = [1-(1-x)^D]/x \quad (5)$$

where  $C_c$  and  $C_l$  are the concentration of the element in the sulfide and the liquid, respectively,  $D$  is the partition coefficient of the element into sulfide, and  $x$  is the weight fraction of sulfide that has segregated.  $C_c/C_l$  will be referred to as the enrichment factor in the text below. Ni and Cu have similar partition-coefficients into sulfide (Rajamani & Naldrett 1978, Peach *et al.* 1989). Experimental work suggests a  $D$  of approximately 200 for rocks of this composition (Rajamani & Naldrett 1978), whereas Peach *et al.* (1989) have calculated  $D$  to be 864 and 1300 for Ni and Cu, respectively, in MORB. If it is assumed that the upper-zone sulfides segregated from the initial liquid, then the enrichment factor of Ni and Cu in the sulfide would be 59 and 206, respectively (Table 7). This raises a problem, because the similarity in the partition coefficients of Ni and Cu requires that they have a similar enrichment-factor in the sulfide. A solution to this problem can be found if it is remembered that the lithophile elements suggest that the trapped liquid in the olivine cumulates was fractionated. If we allow fractionation of 9.8% olivine and 0.2% chromite, the Ni and Ir content of the liquid will have fallen, and the Cu and Pd content risen, such that the enrichment factors all fall in the range 100 to 170 (Table 7), which suggests that between 0.5 and 1% sulfide segregated from the liquid (Fig. 10).

The modeling of the chalcophile and siderophile elements of the lower-zone rocks presents more of a challenge. Elements such as Ni, Co, Os, Ir and Ru have enrichment factors of 10 to 150 relative to the liquid after 20% fractionation (Table 7). The figure of 20% fractionation was chosen because this is the maximum amount of fractionation indicated by the lithophile elements in the lower-zone rocks. Use of the partition coefficients listed in Table 5 and the curves on Figure 10 implies the segregation of about 1% sulfide. However, elements such as Cu, Se, Rh, Pt and Pd have enrichment factors of 300 to 1274 (Table 7), and this implies segregation of approxi-

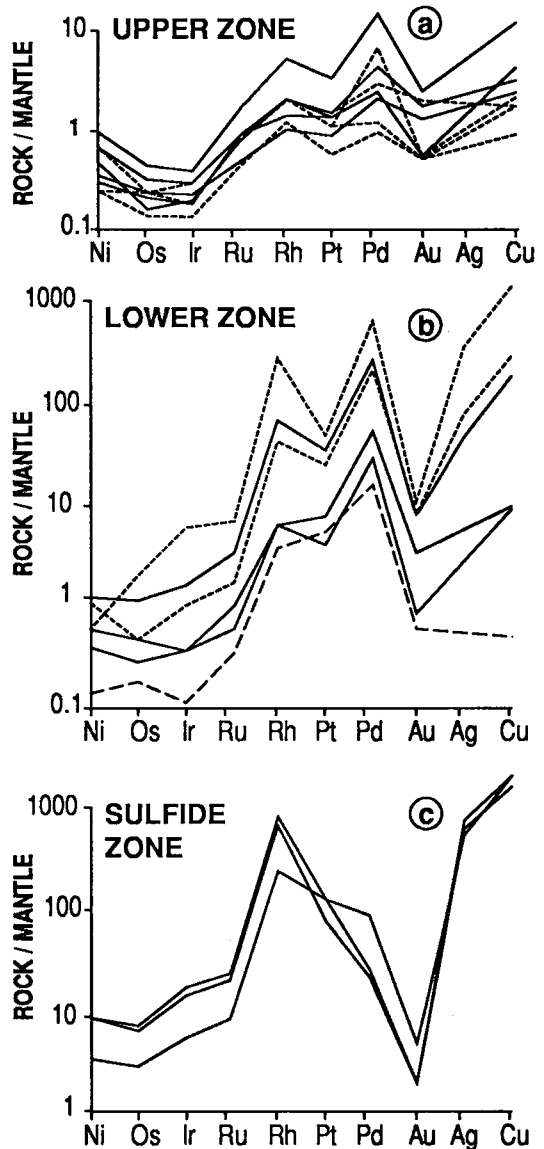


FIG. 8. Mantle-normalized metal patterns, with normalization values from Barnes *et al.* (1988). On a and b, dotted lines: pyroxenite, solid lines: olivine cumulate, dashed line: gabbro.

mately 0.1% sulfide (Fig. 10). Unless some unknown process has disturbed the partition coefficients, it does not seem possible to generate these sulfides simply by segregation from a basaltic komatiite liquid.

In order to make the enrichment factors for Ni, Ir, Os, Ru and Co agree with those for Se, Rh, Pt, Pd, Ag and Cu, the liquid must either contain an order of magnitude less Ni, Ir, Os, Ru and Co, or an order of magnitude more Se, Rh, Pt, Pd, Ag and

TABLE 7. COMPOSITION OF THE BRAVO SULFIDES AND THE DEGREE OF ENRICHMENT IN THE SULFIDES

	Bravo			Enrichment Factor Fractionated Liquid					
	Upper Zone	Lower Zone	Chlorite Sulfide	Upper Zone	Lower Zone	F=0.9	F=0.8	F=0.7	
	1.	2.	3.	4.	5.				
Fe %	52.0	47.0	45.3						
Ni	5.7	2.9	2.5	101	64	560	448	342	
Cu	1.4	10.2	11.3	197	1274	71	80	91	
S	40.3	39.9	40.3						
Ag ppm	<27	16	21.3	<187	94	0.16	0.17	0.21	
As	<11	4.9	3.1	<25	9	0.44	0.50	0.57	
Co	761	1201	1300	9	14	84	84	84	
Sb	26.4	18	1.5	240	150	0.11	0.12	0.14	
Se	<55	121	141	<323	605	0.17	0.2	0.22	
Os ppb	44	46	44	73	92	0.6	0.5	0.4	
Ir	71	77	99	118	154	0.6	0.5	0.4	
Ru	225	177	186	40	28	5.5	6.2	7.1	
Rh	218	802	971	114	381	1.9	2.1	2.4	
Pt	1132	3451	1912	107	290	10.5	11.9	13.5	
Pd	2671	14680	571	172	838	15.5	17.5	20	
Au	162	143	11	202	158	0.8	0.9	1	

1. Composition of sulfide in the upper zone calculated from bv6.
2. Composition of sulfide in the lower zone calculated from bv14 and 16
3. Composition of sulfide in the chlorite-sulfide rock from bv2, 5 and 15
4. Enrichment factor of the element in the upper-zone sulfide assuming that the liquid has experienced 10% olivine fractionation.
5. Enrichment factor of the element in the lower-zone sulfide assuming that the liquid has experienced 20% olivine fractionation.

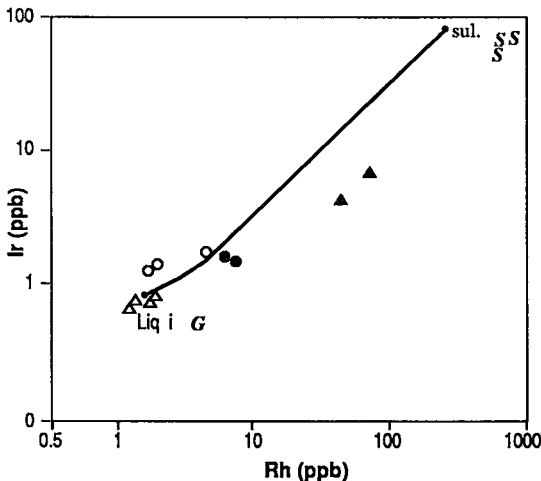


FIG. 9. Ir versus Rh; legend as in Fig. 4. Note that the upper-zone samples plot close to a tie-line between the initial liquid (average of BV 3, 4 and 11) and sulfide from the upper zone in equilibrium with this liquid (based on BV6), whereas the lower-zone samples lie on the Rh-enriched side of the tie-line and the sulfide (S) contains an order of magnitude more Rh.

Cu than estimated. To propose a lowering of Ni, Ir, Os, Ru and Co concentrations in the silicate liquid would only work with absurdly low concentrations

in these elements (e.g., 40 ppm Ni). It might, however, be possible to raise the concentration of Se, Rh, Pt, Pd, Ag and Cu by contamination of the magma. Because of the high temperature of komatiitic magmas, contamination of the magma by the enclosing sediments may have occurred (Huppert & Sparks 1985). However, the dolomitic quartzite (BV 13, Table 3) at the base of the Bravo intrusion does not contain sufficient Cu, Pt, Pd and Rh to act as a source of these elements. The similarity in the ratio of incompatible elements of the upper and lower zone requires that any contaminant not disturb these ratios. Effectively this constraint rules out contamination by the greywackes in the area, since these have high Zr/Y and LREE/HREE ratios and high Th concentrations (CT 61, Table 3). The partial melting of the sulfides in the greywackes could produce a suitably Cu-rich contaminant, but this would require temperatures of greater than 850°C (Craig & Kullerud 1969), and at these temperatures the silicate component of the greywacke should also have melted, which, as pointed out above, would have disturbed the lithophile elements.

One possible contaminant that might fulfill the requirements would be a Cu-rich sulfide melt. Two possible sources of such a melt would be: a) the partial melt of a pre-existing sulfide (Brüggmann *et al.* 1989), b) a fractionated sulfide liquid formed during the crystallization of a sulfide magma (Naldrett *et al.* 1982). The residual liquid or the partial melt

of a komatiitic sulfide could contain up to 40% Cu (Fig. 3 of Craig & Kullerud 1969). Contamination of the komatiitic magma with 0.25% of such a sulfide would increase the Cu content of the silicate liquid to 1000 ppm, and hence change the enrichment factor of Cu in the sulfides from 1200 to 120, *i.e.*, similar to that observed for Ni. If it is argued that Rh, Pd, Pt and Ag are incompatible with the pyrrhotite residual phase of a massive sulfide, then the concentration of these elements would also be expected to be high in the partial melt or fractionated liquid. Hence a partial melt or a fractionated liquid of a pre-existing sulfide may have acted as a source to contaminate the subsequent komatiitic magma that formed Bravo.

## MODEL AND CONCLUSIONS

The Bravo intrusion represents an interesting case-study, in that the composition of these rocks appears to have been affected by at least four processes: partial melting, contamination, crystal fractionation and hydrothermal alteration. The field, petrographic and geochemical evidence may be interpreted as follows.

After the rifting phase of the Cape Smith Belt and the development of the Povungnituk Group, komatiitic magma derived by approximately 25% batch partial melting of a primitive mantle rose into crust, leaving olivine, low-Ca pyroxene and garnet in the source. The komatiite magma created a system of sills and dykes in the Povungnituk Group,

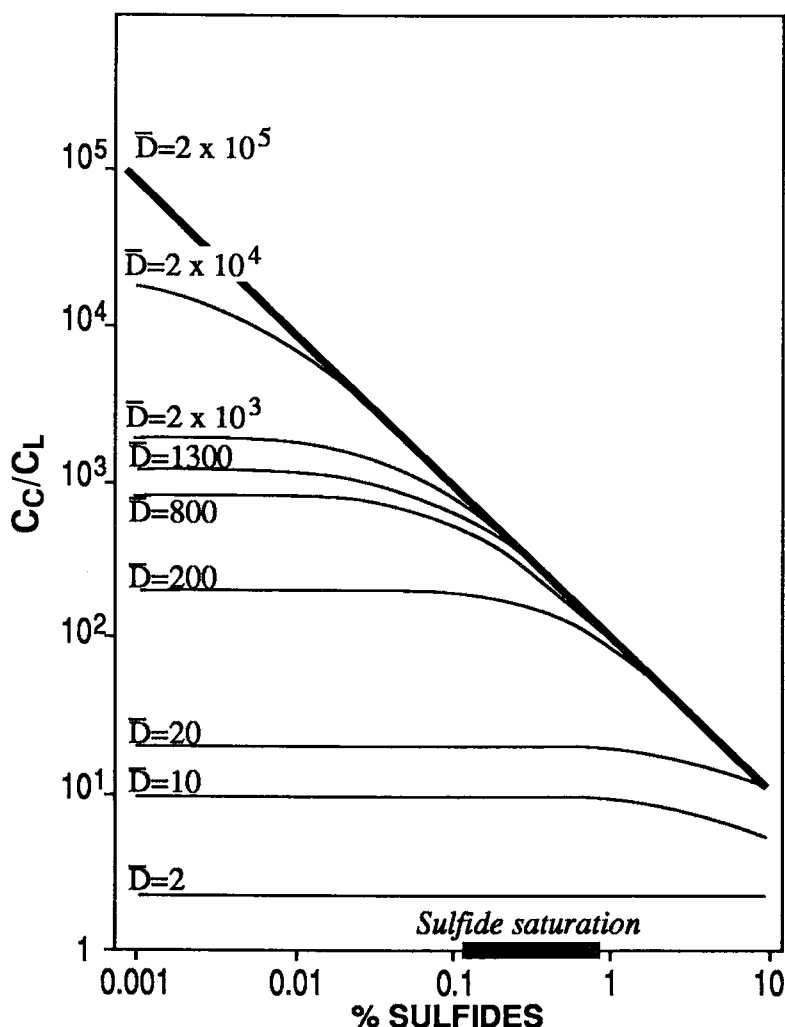


FIG. 10. Enrichment factor *versus* % sulfides segregated for partition coefficients ranging from 2 to 20,000, calculated using equation 5.

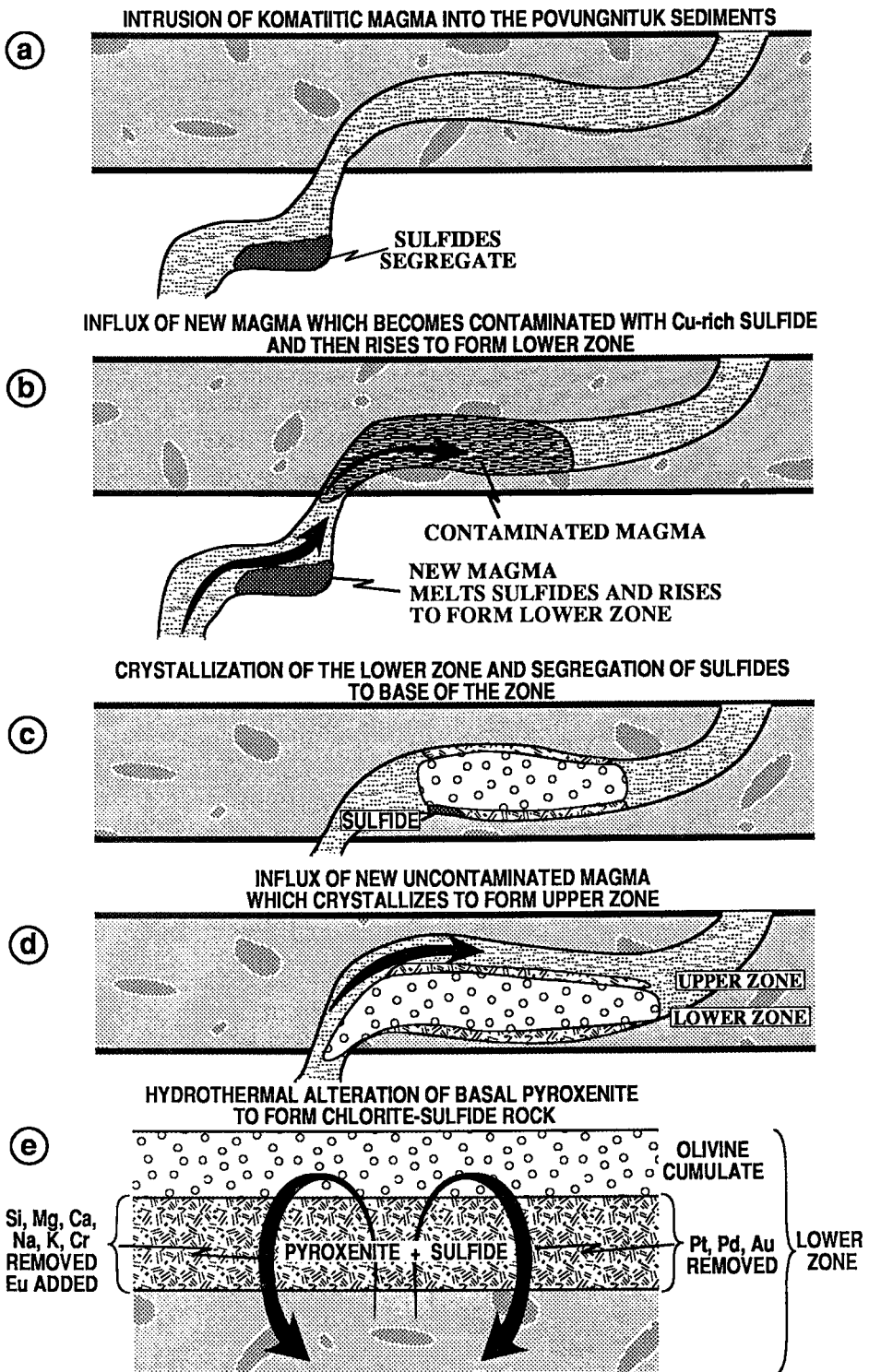


Fig. 11. Model for the formation of the Bravo sill. See text for further explanations.

now represented by the Delta Horizon, which may be thought of as a conduit to the overlying Chukotat lavas (Giovenazzo *et al.* 1989). The PGE-rich nature of the sulfide associated with the komatiites of the Cape Smith Belt is in part due to the high degree of partial melting involved in forming the komatiite magma; at high degrees of partial melting, no sulfide remains in the source, and therefore all the Pt and Pd in the source is released to the magma.

In the region of the Bravo Sill, a batch of komatiite magma became sulfide-saturated. The sulfide collected the siderophile and chalcophile elements and settled out of the magma to form a pool of sulfide liquid (Fig. 11a). A new influx of magma passed over this sulfide and was contaminated by a Cu-rich sulfide liquid derived either by partial melting of the solidified sulfide or by crystal fractionation of the sulfide. This sulfide melt, rich in Cu, Pd, Pt and Rh, mixed into the komatiite and changed Ni/Cu, Pd/Ir and other interelement ratios (Fig. 11b). The contaminated magma was then emplaced in the Bravo region, where upon crystallization it formed the lower zone of the sill by olivine accumulation and sulfide segregation (Fig. 11c).

A new influx of uncontaminated komatiitic magma was subsequently emplaced, and this magma, upon cooling, crystallized to form the olivine cumulates of the upper zone (Fig. 11d). As the cumulates contain 40 to 60% cumulate olivine, mass-balance considerations dictate that some fractionated liquid must have been expelled, perhaps eventually rising to the surface to form part of the Chukotat lavas.

Portions of the sulfide-rich basal pyroxenite underwent intense alteration by a fluid containing a "soft" ligand, resulting in the loss of Si, Mg, Ca, Na, K, Cr, Pt, Pd and Au, and the introduction of Eu (Fig. 11d).

#### ACKNOWLEDGEMENTS

We thank the Ministère de l'Énergie et des Ressources du Québec, who financed the field work and the salary of D. Giovenazzo, Falconbridge Ltd. for logistical support, NSERC for covering the cost of analytical work, C. Dellaire for drafting, R. Lechausser for assistance in determining the PGE, Professor E.W. Sawyer for reading early drafts of the manuscript, Professor J. Guha for advice in the development of the project, and two anonymous referees for careful reviews of the manuscript.

#### REFERENCES

- BARNES, S.-J. (1987): Unusual nickel and copper to noble-metal ratios from the Råna layered intrusion, northern Norway. *Nor. Geol. Tidsskr.* **67**, 215-231.
- \_\_\_\_\_, BOYD, R., KORNELIUSSEN, A., NILSSON, L.-P., OFTEN, M., PEDERSEN, R.-B. & ROBINS, B. (1988): The use of mantle normalization and metal ratios in discriminating between the effects of partial melting, crystal fractionation and sulphide segregation on platinum-group elements, gold, nickel and Cu: examples from Norway. In *Geo-platinum 87 Symp.* Vol. (H.M. Prichard, P.J. Potts, J.F.W. Bowles & S.J. Cribbs, eds.). Elsevier, London (113-143).
- \_\_\_\_\_ & OFTEN, M. (1990): Ti-rich komatiites from northern Norway. *Contrib. Mineral. Petrol.* **105**, 42-54.
- BARNES, S.J., NALDRETT, A.J. & COATS, C. (1982): Petrogenesis of a Proterozoic nickel sulfide - komatiite association: the Katinik Sill, Ungava, Quebec. *Econ. Geol.* **77**, 413-429.
- BÉDARD, J.H., FRANCIS, D.M., HYNES, A. & NADEAU, S. (1984): Fractionation in the feeder system at a Proterozoic rifted margin. *Can. J. Earth Sci.* **21**, 489-499.
- BESWICK, A.E. (1982): Some geochemical aspects of alteration and genetic relations in komatiitic suites. In *Komatiites* (N.T. Arndt & E.G. Nisbet, eds.). Allen & Unwin, London (283-308).
- BRÜGMANN, G.E., ARNDT, N.T., HOFFMANN, A.W. & TOBSCHALL, H.J. (1987): Noble metal abundances in komatiite suites from Alexo, Ontario, and Gorgona Island, Colombia. *Geochim. Cosmochim. Acta* **51**, 2159-2169.
- \_\_\_\_\_, NALDRETT, A.J. & MACDONALD, A.J. (1989): Magma mixing and constitutional zone refining in the Lac des Iles Complex, Ontario: genesis of platinum-group element mineralization. *Econ. Geol.* **84**, 1557-1573.
- CAMPBELL, I.H. & NALDRETT, A.J. (1979): The influence of silicate:sulfide ratio on the geochemistry of the magmatic sulfides. *Econ. Geol.* **74**, 1503-1505.
- CRAIG, J.R. & KULLERUD, G. (1969): Phase relations in the Cu-Fe-Ni-S system and their application to magmatic ore deposits. *Econ. Geol., Monogr.* **4**, 344-358.
- CROCKET, J.H. (1981): Geochemistry of the platinum-group elements. In *Platinum-Group Elements: Mineralogy, Geology, Recovery* (L.J. Cabri, ed.). *Can. Inst. Min. Metall., Spec. Vol.* **23**, 47-64.
- \_\_\_\_\_ & MACRAE, W.E. (1986): Platinum-group element distribution in komatiitic and tholeiitic volcanic rocks from Munro Township, Ontario. *Econ. Geol.* **81**, 1242-1251.
- DAXL, H. (1988): *The Platinum-Group Element Occurrences of the Kenty Lake Area, Ungava Trough, New Quebec*. M.Sc. thesis, Queen's Univ., Kingston, Ontario.

- DILLON-LEITCH, H.C.H., WATKINSON, D.H. & COATS, C. (1986): Distribution of platinum-group elements in the Donaldson West deposit, Cape Smith Fold Belt, Quebec. *Econ. Geol.* **81**, 1147-1159.
- FRANCIS, D.M., HYNES, A.J., LUDDEN, J. & BÉDARD, J. (1981): Crystal fractionation and partial melting in the petrogenesis of a Proterozoic high-MgO volcanic suite, Ungava, Quebec. *Contrib. Mineral. Petrol.* **78**, 27-36.
- \_\_\_\_\_, LUDDEN, J. & HYNES, A. (1983): Magma evolution in a Proterozoic rifting environment. *J. Petrol.* **24**, 556-582.
- GIOVENAZZO, D., PICARD, C. & GUHA, J. (1989): Tectonic setting of Ni-Cu-PGE deposits in the central part of the Cape Smith Belt. *Geosci. Can.* **16**, 134-136.
- HUPPERT, H.E. & SPARKS, R.S.J. (1985): Cooling and contamination of mafic and ultramafic lavas during ascent through continental crust. *Earth Planet. Sci. Lett.* **74**, 371-386.
- HYNES, A. & FRANCIS, D.M. (1982): A transect of the Early Proterozoic Cape Smith foldbelt. *Tectonophysics* **88**, 23-59.
- IRVING, A.J. (1978): A review of experimental studies of crystal/liquid trace element partitioning. *Geochim. Cosmochim. Acta* **42**, 743-770.
- JONES, J.H. (1984): Temperature- and pressure-independent correlations of olivine/liquid partition coefficients and their application to trace element partitioning. *Contrib. Mineral. Petrol.* **88**, 126-132.
- KEAYS, R.R. (1982): Palladium and iridium in komatiites and associated rocks: application to petrogenetic problems. In *Komatiites* (N.T. Arndt & E.G. Nisbet, eds.), Allen & Unwin, London (435-458).
- LAMOTHE, D., GIOVENAZZO, D. & PICARD, C. (1987): Platinum-group element occurrences in the Ungava Trough, New Quebec. *Ministère de l'Énergie et des Ressources du Québec, Document de promotion* **15**.
- LESHER, C.M. & KEAYS, R.R. (1984): Metamorphically and hydrothermally mobilized Fe-Ni-Cu sulfides at Kambalda, Western Australia. In *Sulphide Deposits in Mafic and Ultramafic Rocks* (D. Buchanan & M. Jones, eds.). Inst. Min. Metall., London (62-69).
- LUDDEN, J., GÉLINAS, L. & TRUDEL, P. (1983): Archean metavolcanics from the Rouyn district, Abitibi Greenstone Belt, Quebec. 2. Mobility of trace elements and petrogenetic constraints. *Can. J. Earth Sci.* **19**, 2276-2287.
- MORGAN, J. (1986): Ultramafic xenoliths: clues to earth's late accretionary history. *J. Geophys. Res.* **91**, 12375-12387.
- NALDRETT, A.J. (1981): Nickel sulfide deposits: classification, composition and genesis. *Econ. Geol., 75th Anniv. Vol.*, 628-655.
- \_\_\_\_\_, & BARNES, S.-J. (1986): The behavior of platinum-group elements during fractional crystallization and partial melting with special reference to the composition of magmatic sulfide ore. *Fortschr. Mineral.* **64**, 113-133.
- \_\_\_\_\_, INNES, D.G., SOWA, J. & GORTON, M.P. (1982): Compositional variations within and between five Sudbury ore deposits. *Econ. Geol.* **77**, 1519-1534.
- NIELSEN, R.L. (1985): EQUIL: a program for the modelling of low-pressure differentiation-processes in natural mafic bodies. *Comput. Geosci.* **11**, 531-546.
- PARRISH, R.R. (1989): U-Pb geochronology of the Cape Smith Belt and Sugluk Block, northern Quebec. *Geosci. Can.* **16**, 126-129.
- PEACH, C.L., MATHEZ, E.A. & KEAYS, R.R. (1989): Sulfide melt - silicate melt distribution coefficients for the noble metals as deduced from MORBs. *Bull. Geol. Soc. Finland* **61**(1), 58 (abstr.).
- PHILLIPS, G.N. & GROVES, D.I. (1983): The nature of Archaean gold-bearing fluids as deduced from gold deposits of western Australia. *J. Geol. Soc. Aust.* **30**, 25-39.
- PICARD, C. (1986): Lithogéochimie de la partie centrale de la Fosse de l'Ungava. *Ministère de l'Énergie et des Ressources du Québec, DV* **86-16**, 57-72.
- \_\_\_\_\_, & GIOVENAZZO, D. (in press): Pétrographie, géochimie et gîtologie des roches plutoniques ultramafiques et mafiques protérozoïques de la partie centrale de la Fosse de l'Ungava: implications sur la distribution des éléments du groupe des platinoïdes. *Ministère de l'Énergie et des Ressources du Québec*.
- \_\_\_\_\_, LAMOTHE, D., PIBOULE, M. & OLIVER, R. (in press): Magmatic and geotectonic evolution of a Proterozoic oceanic basin system: the Cape Smith Thrust-Fold Belt (New Quebec). *Precambrian Res.*
- PLIMER, I.R. & WILLIAMS, P.A. (1988): New mechanisms for the mobilization of the platinum-group elements in the supergene zone. In *Geo-platinum 87 Symp. Vol.* (H. M. Prichard, P.J. Potts, J.F.W. Bowles & S.J. Cribbs, eds.). Elsevier, London (83-92).
- RAJAMANI, V. & NALDRETT, A.J. (1978): Partitioning of Fe, Co, Ni and Cu between sulfide liquid and basaltic melts and the composition of Ni-Cu sulfide deposits. *Econ. Geol.* **73**, 82-93.
- ROBERT, R.V.D., VAN WYK, E. & PALMER, R. (1971): Concentration of the noble metals by a fire assay

- technique using nickel sulfide as the collector. *Nat. Inst. Metall., Rep.* **1371**, 1-14.
- ROEDER, P.L. & EMSLIE, R.F. (1970): Olivine-liquid equilibrium. *Contrib. Mineral. Petrol.* **29**, 275-282.
- ROWELL, W.F. & EDGAR, A.D. (1986): Platinum-group mineralization in a hydrothermal Cu-Ni sulfide occurrence, Rathbun Lake, northeastern Ontario. *Econ. Geol.* **81**, 1272-1277.
- SAMIS, A.N. & ANDERSEN, E.O. (1980): 1979 Year end report Kenty Project, Summary of 1979 exploration programme on Ungava permits 567 and 568. *Ministère de l'Énergie et des Ressources du Québec, Doc. Tech.* **GM 36257**.
- SEWARD, T.M. (1973): Thio complexes of gold and the transport of gold in hydrothermal ore solutions. *Geochim. Cosmochim. Acta* **37**, 379-399.
- SUN, SHEN-SU & NESBITT, R. (1978): Petrogenesis of Archaean ultrabasic and basic volcanics: evidence from rare earth elements. *Contrib. Mineral. Petrol.* **65**, 301-325.
- TAKAHASHI, E. (1986): Melting of dry peridotite KLB-1 up to 14 GPa: implications on the origin of peridotitic upper mantle. *J. Geophys. Res.* **91**, 9367-9382.
- TAYLOR, S.R. & MCLENNAN, S.M. (1985): *The Continental Crust: its Composition and Evolution*. Blackwell, Oxford, England.
- TREMBLAY, C. (1990): *Les éléments du groupe du platine dans le dyke de Méquillon, ceinture de Cape Smith, Nouveau-Québec*. Mémoire de maîtrise, Univ. Québec, Chicoutimi, Québec.
- \_\_\_\_\_ & BARNES, S.-J. (1989): Platinum-group elements in the Méquillon dyke, Ungava Trough, New Quebec. *Geol. Assoc. Can. - Mineral. Assoc. Can., Abstr. Program* **14**, A79.
- WESTLAND, A.D. (1981): Inorganic chemistry of the platinum-group elements. In *Platinum-Group Elements: Mineralogy, Geology, Recovery* (L.J. Cabri, ed.). *Can. Inst. Min. Metall., Spec. Vol.* **23**, 5-18.
- WOOD, S.A., MOUNTAIN, B.W. & FENLON, B. (1990): Thermodynamic constraints on the solubility, transport, and deposition of platinum and palladium in hydrothermal solutions: reassessment of hydroxide, bisulfide and ammonia complexing. *Econ. Geol.* **85**, 2020-2028.

*Received December 15, 1989, revised manuscript accepted July 30, 1990.*